

## A new approach to dynamic barite sag analysis on typical field oil-based drilling fluid

Titus Ntow Ofei<sup>1</sup>, Bjørnar Lund<sup>2</sup>, Arild Saasen<sup>3</sup>, Sigbjørn Sangesland<sup>1</sup>, Knut Richard Gyland<sup>4</sup>, and Harald Linga<sup>2</sup>

<sup>1</sup>NTNU, Department of Geoscience and Petroleum, Trondheim, Norway

<sup>2</sup>SINTEF, Department of Petroleum, Norway

<sup>3</sup>UiS, Department of Energy and Petroleum Engineering, Stavanger, Norway

<sup>4</sup>M-I SWACO, Schlumberger, Norway

### ABSTRACT

Laboratory and field experiences record that sagging of weighting agents such as barite in drilling fluids is often worse in dynamic conditions, e.g. pumping, tripping or drill pipe rotation, than in static conditions. Barite sag has resulted in problematic wellbore issues including loss of wellbore control, lost circulation, stuck pipe and high torque. Till date, the prediction of barite sag in dynamic condition is still a challenge in the industry. An indirect measurement protocol to examine the effects of shear rate and viscosity on dynamic barite sag of drilling fluids is proposed. This study presents an experimental analysis of dynamic barite sag phenomenon on a typical oil-based drilling fluid sample. All rheometry and dynamic barite sag tests were conducted at 50°C using an advanced Anton Paar rheometer MCR 102/302 with either the smooth or grooved bob-in-cup measuring system. The viscoelastic properties which are related to the microstructural building/breakdown of the fluid sample were investigated under oscillatory amplitude and frequency sweeps. The dynamic sag was measured under steady and oscillatory low to ultra-low shear rates from 5.11 to 0.001 s<sup>-1</sup> to closely compare to sag-prone conditions during drilling operation. Preliminary results indicate a strong dependence of barite sag on shear rate above a critical shear rate value of 0.1 s<sup>-1</sup>. Furthermore, with higher viscosity, less dynamic sag is observed.

### INTRODUCTION

The settling and sagging of weighting materials, such as barite in drilling fluids is a major concern when drilling and completing a well. Barite sag is caused by settling of suspended particles in the lower side of the borehole which can lead to variation in drilling fluid density. Several wellbore problems that result from barite sag include fluctuation in torque and drag loads, difficulty in running of casing, displacement inefficiency during cementing operation, loss circulation, stuck pipe, well and pressure control related issues, among others.<sup>1-4</sup> Omland et al.,<sup>5</sup> reviewed different techniques available for detecting particle sagging in drilling fluids which ranged from the standard viscometer to lab-scale flow loops and observed that the methods were promising to detecting sag potential in drilling fluids. A few studies reported results from lab-scale flow loops to examine the sag potential in static and dynamic conditions. Skalle et al.,<sup>4</sup> built an inclined sag tester of length 1.5 m fixed unto a vertical collector pipe to study the effect of rheology on particle settling and sagging in both static and dynamic conditions. The difference in pressures between the bottom of the inclined pipe and the collector pipe determines whether the drilling fluid is stable or unstable. Dye et al.,<sup>6</sup> investigated the effect of shear rate on dynamic barite sag for invert-emulsion drilling fluids using a field

viscometer capable of measuring at  $0.0017\text{ s}^{-1}$  and an eccentric wellbore-hydraulics flow loop of about 2 m length. The study concluded that dynamic barite sag increased as hole angle increased from  $45\text{-}60^\circ$  while the onset of dynamic sag occurred at shear rates less than  $4\text{ s}^{-1}$ . A high angle sag test (HAST) device capable of characterizing sag signatures by the movement of the centre of mass of the test fluid at temperatures up to  $300^\circ\text{F}$  and deviation angle from  $20^\circ$  to  $90^\circ$  was designed.<sup>7</sup> The study concluded that viscosity parameters of drilling fluids are unreliable measures for predicting sag performance in extended reach drilling. Marshall,<sup>8</sup> reported a laboratory study on oil-based drilling fluids where seven companies participated using their in-house instruments. The company involved were Grace, Anton Paar, Brookfield, Malvern, OFITE, Baker Hughes, and Kelco oilfield group. Viscosity measurement of the base fluid indicate that there was broad agreement among the seven instruments, particularly at intermediate shear rates. Nonetheless, repeatability of the measurements revealed that only two instruments (Anton Paar and Malvern), of which are most expensive and sophisticated, produced numbers close to the theoretically expected results over large range of shear rate.

In this study, the Anton Paar rheometer and density meter are used to examine the effects of shear rate and viscosity on dynamic barite sag potential in typical oil-based drilling fluid.

## MATERIALS AND METHOD

### Fluid composition and mixing

A referenced oil-based drilling fluid (OBDF) composition with oil/water ratio of 80/20, which consists of base oil,  $\text{CaCl}_2$  brine, lime, emulsifier, viscosifiers, fluid loss agent, low gravity  $\text{CaCO}_3$ , and API barite, is defined in Table 1. All the fluid components were provided by Schlumberger M-I SWACO, Norway. The OBDF sample was

mixed using the Waring blender at a speed of 6000 rpm for a total of 88 minutes. The mixing procedure started by placing a container of base oil in a cooling bath to maintain the temperature below  $65^\circ\text{C}$ . Afterwards, the emulsifier, viscosifiers, lime, fluid loss agent,  $\text{CaCl}_2$ ,  $\text{CaCO}_3$ , and API barite were added in varying concentrations, as shown in Table 1. The electrical stability and specific gravity of the sample were measured as 687 volts and 1.43 respectively.

Table 1. Composition of referenced OBDF

Product	Concentration (g/l)	Mixing time (min.)
Mineral oil	501.9	-
Emulsifier	20.0	2
Viscosifier (low temp)	9.0	4
Viscosifier (high temp)	13.0	4
Lime	20.0	5
Fluid loss agent	10.0	5
$\text{CaCl}_2$ brine	199.3	15
$\text{CaCO}_3$ (low gravity)	50.0	10
API barite	610.8	25

### Fluid characterization

An advanced rheometer, Anton Paar MCR 102 using a couette geometry with smooth bob (CC27) was utilised to conduct the rheological measurements on the OBDF at  $50^\circ\text{C}$ . The various rheological tests performed include, flow curves, oscillatory amplitude sweep, oscillatory frequency sweep, and steady and oscillatory time tests.

The flow curves were measured under a controlled shear rate and show the viscosity function of the sample. The sample was pre-sheared at a constant shear rate of  $1000\text{ s}^{-1}$  for 200 s before linearly ramping down the shear rate from 1000 to  $1\text{ s}^{-1}$  for 100 measuring points with 2 s measuring point duration. To understand the flow characteristics in the low shear rate region, the shear rate was logarithmically ramped up from 0.001 to  $1\text{ s}^{-1}$  for 40 measuring points with 2 s measuring point duration. To examine the thixotropy behaviour of the

sample, the shear rate was again linearly ramped up from 1 to 1000  $s^{-1}$  for a total of 100 measuring points.

The amplitude sweep tests which uses sinusoidal oscillations allows the testing of the microstructure of the sample without breaking the sample structure.<sup>9</sup> The test was carried out with a constant angular frequency of 10  $rad/s$  and increasing strain amplitude from 0.001 to 100% at a slope of 5 measuring points per decimal, accounting to 26 measuring points. The limit of the linear viscoelastic (LVE) region, below which the measured properties of the sample are non-destructive, is determined for use as a parameter for the frequency sweep test. The test also measures the storage modulus ( $G'$ ), characterising the material's elastic behaviour, and loss modulus ( $G''$ ), characterising the viscous behaviour of the material. The flow point, where  $G' = G''$ , is measured as the point where the material's microstructure deforms and initiates flow. If  $G' > G''$ , the elastic behaviour dominates the viscous behaviour and the sample depicts a solid-like character. Conversely,  $G'' > G'$ , indicates that the viscous behaviour dominates the elastic behaviour of the sample and shows a liquid-like character.

The frequency test also uses sinusoidal oscillations at small strain amplitudes usually within the LVE region.<sup>9</sup> A shear strain amplitude within the LVE region was applied on the sample over a decreasing range of angular frequency from 100 to 0.001  $rad/s$  at a slope of 5 measuring points per decimal, amounting to 26 measuring points. The comparison of  $G'$  and  $G''$  is of greater importance at lower frequencies where dynamic sag is more likely to occur. The phase shift angle,  $\delta$ , of the sample, which is indicative of ideal solid behaviour at  $0^\circ$  and purely liquid behaviour at  $90^\circ$  is measured to evaluate the viscoelastic behaviour of the fluid sample. Similarly, the damping factor,  $\tan(\delta) = G''/G'$ , which indicates whether the sample is more viscous when  $\tan(\delta) > 1$ , or more elastic when  $\tan(\delta) < 1$  is

measured. It also defines the gel properties of the fluid sample.<sup>2</sup>

During the steady time test, the viscosity of the sample was measured at a constant shear rate in isothermal condition for a fixed length of time. The constant shear rates used are 5.11, 1.703, 0.10, and 0.001  $s^{-1}$ . The total length of time was 4000 s for all shear rates at  $50^\circ C$  for 1000 measuring points.

For the oscillatory time test, both strain amplitude and angular frequency were held constant. An angular frequency of 5.11  $rad/s$  and strain amplitude of 1% were selected and the experiment was run for a total time of 4000 s at 1000 measuring points with 4 s interval. An isothermal condition of  $50^\circ C$  was imposed.

By oscillatory shear test, certain parameters have been adopted from classic mechanics to measure the rheological properties of the viscoelastic fluid. The shear modulus  $G$ , under uniaxial stress conditions, according to Hooke's law, is constant for perfectly elastic material. However, for oscillatory stresses, a complex shear modulus,  $G^*$ , which is divided into a storage modulus,  $G'$ , and a loss modulus,  $G''$ , is defined by the following equations:<sup>10</sup>

$$G^* = \frac{\tau_A}{\gamma_A}, \quad (1)$$

$$G' = |G^*| \cos(\delta) = \frac{\tau_A}{\gamma_A} \cos(\delta), \quad (2)$$

$$G'' = |G^*| \sin(\delta) = \frac{\tau_A}{\gamma_A} \sin(\delta), \quad (3)$$

where  $\tau_A$  in (Pa), is the stress amplitude,  $\gamma_A$  (%) is the strain amplitude, and  $\delta$  is the phase shift angle between  $G''$  and  $G'$ .

#### Dynamic barite sag test

The testing of the dynamic barite sag of the fluid sample was carried out using the advanced Anton Paar rheometer MCR 302

and Anton Paar density meter DMA 5000 M. After mixing the fluid components, its initial density,  $\rho_{initial}$ , was measured using the digital density meter DMA 5000 M with a tolerance of  $\pm 5 \times 10^{-5} \text{ g/cm}^3$ . It is based on a U-tube principle which measures the inertial mass of a known sample volume. The fluid sample is filled into a U-shaped tube that is mounted on a counter mass using a syringe. The U-tube is then excited and starts to oscillate. The change in frequency is then measured and the density can be determined.<sup>11</sup> The instrument performs several measurements automatically. For a single sample entry, three series of measurements were taken after which the average value of these measurements was calculated.

The grooved bob-in-cup measuring system of the Anton Paar rheometer MCR 302 was used to investigate the dynamic barite sag of the fluid sample at a constant temperature of 50°C. Drilling fluid sample of ~20 mL was poured into the measuring cup. The constant shear rate method was imposed where for each fixed shear rate, the viscosity was measured over a time period of 4000 s. At the end of each run, ~3 mL of the fluid sample was taken from the top of measuring cup using a syringe and its density,  $\rho_{top}$ , measured via the density meter. The dynamic sag density was calculated as:

$$\rho_{sag} = \rho_{initial} - \rho_{top} \quad (4)$$

The sag factor,  $SF$ , was also computed as:

$$SF = \frac{\rho_{initial}}{\rho_{initial} + \rho_{top}} \quad (5)$$

For a fluid to exhibit excellent suspension characteristics, the sag factor should be 0.50. Nonetheless, a fluid which has a sag factor greater than 0.53 is considered to have inadequate suspension properties.<sup>12</sup>

## RESULTS AND DISCUSSION

Viscoelastic rheometry measurements such as flow curves, amplitude and frequency sweeps, as well as dynamic barite sag measurements of the drilling fluid under steady and oscillatory conditions are presented in this section.

### Flow curves

Fig. 1 illustrates the flow curve in the form of shear stress vs shear rate, whereas Fig. 2 presents the viscosity vs shear rate of the oil-based drilling fluid sample at 50°C. Results from Fig. 1 indicate a shear-thinning behaviour of the drilling fluid sample. The gap between the ramping up and ramping down curves (see inset of Fig. 1) demonstrates the thixotropic behaviour of the drilling fluid. Similar phenomenon was reported by Maxey<sup>13</sup>.

The viscosity profile of the fluid sample shown in Fig. 2 is divided into three distinct features; the upper Newtonian region characterized by a finite viscosity between 0.001 to 0.1  $\text{s}^{-1}$ , the power law or nonlinear region between 0.1 to 0.1 and 100  $\text{s}^{-1}$ , and the lower Newtonian region characterized by a nearly-constant finite viscosity between 500 to 1000  $\text{s}^{-1}$ . The viscosity profile decreases with increasing shear rate, thus exhibiting a shear-thinning behaviour. It can be observed that the rate at which viscosity increases as shear rate decreases is likely a probability of sag events being witnessed with the fluid sample. The fluid's upper Newtonian viscosity (below 0.1  $\text{s}^{-1}$ ) may exhibit strong gels that can minimize sag events.

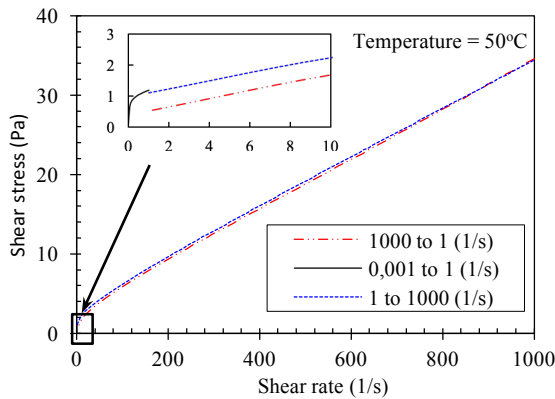


Figure 1. Shear stress vs. shear rate flow curve for the sample fluid system at 50°C showing the thixotropic behaviour at low shear rates.

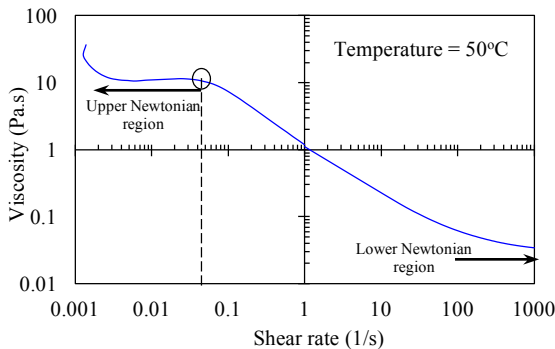


Figure 2. Viscosity vs. shear rate profile for the sample fluid system at 50°C showing the upper, lower Newtonian and nonlinear regions.

Amplitude sweep

The measuring results of the amplitude sweeps compare the storage modulus,  $G'$ , and loss modulus,  $G''$ , of the fluid sample as presented in Fig. 3 and Fig. 4 with shear strain and shear stress respectively. Results in Fig. 3 shows that the drilling fluid sample is predominantly elastic within the LVE region since  $G' > G''$ . The values of  $G'$  indicates that part of the induced energy by the external stress is temporarily stored during the test to be retrieved upon removal of the stress, whereas,  $G''$  values describe the portion of the deformation energy that is lost by internal friction during shearing. The limit of LVE region occurs at a shear strain of 0.2%. Within this limit, the microstructure of the fluid sample remains undisturbed. Beyond

the LVE region, both  $G'$  and  $G''$  curves drop continuously, thus indicating a gradual breakdown of the superstructure of the fluid sample. The final flow point where  $G' = G''$  occurs at a shear strain of 17.4%. Between the limit of LVE region and the flow point, micro cracks in the fluid sample develop and grow to form a continuous macro crack throughout the entire sample. This situation causes the viscous behaviour of the fluid sample to dominate and the entire sample start to flow at  $G' = G''$ . The fluid structure becomes completely viscoelastic liquid when  $G'' > G'$ .

In Fig. 4, the yield stress,  $\tau_y$ , and flow stress,  $\tau_f$ , values were estimated as 0.1 Pa and 1.248 Pa respectively. The flow transition index,  $\tau_f/\tau_y$ , which describes the transition behaviour from the LVE region to the state of flow is computed as 12.48. A value more than unity indicates that the initial structural strength of the LVE region has already decreased but the sample still predominantly displays the properties of a gel or solid matter.

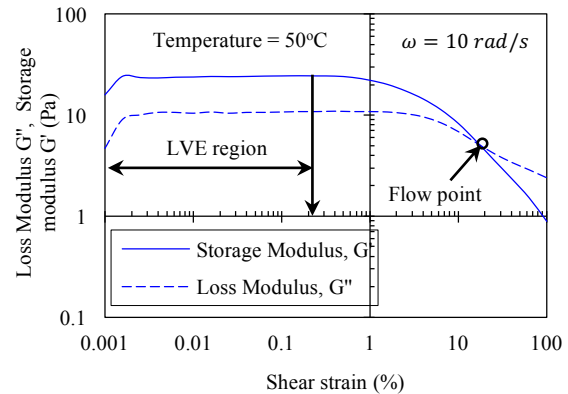


Figure 3. Amplitude sweep presented with shear strain showing the limit of LVE region and flow point at  $G' = G''$ .

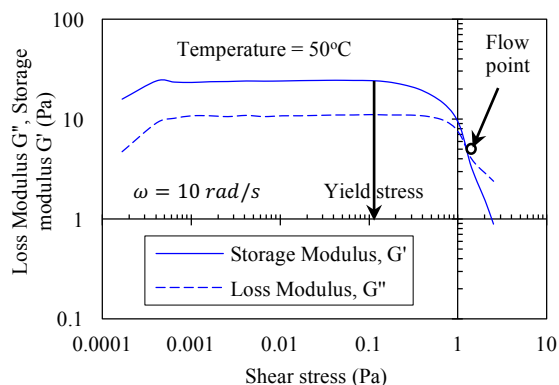


Figure 4. Amplitude sweep presented with shear stress showing the yield stress,  $\tau_y$ , within the limit of LVE region and flow stress,  $\tau_f$ , at  $G' = G''$ .

### Frequency sweep

Results from the frequency test are presented in Fig. 5 and Fig. 6 where the precondition is that the selected shear strain amplitude is within the limit of the LVE region. The fluid sample exhibited a higher storage modulus than the loss modulus during the entire testing period which indicates a stable gel structure as shown in Fig. 5. In addition, the complex viscosity, where the contribution of gel structure is included in the measured viscosity, decreases with increasing angular frequency as presented in Fig. 5. From Fig. 6, the phase shift angle,  $\delta$ , also indicate that the fluid sample shows viscoelastic behaviour as  $\delta$  ranges between 23 and 40. There is more gel structure forming up to  $\omega = 0.4 \text{ rad/s}$  which is characterized by a decline in slope of the curve, whereas a gel structure breakdown is observed above  $\omega = 0.4 \text{ rad/s}$ , with an increasing slope characteristics of the curve. The damping factor curve also shows that the fluid sample is entirely elastic since  $\tan(\delta) < 1$  over the whole range of angular frequency.

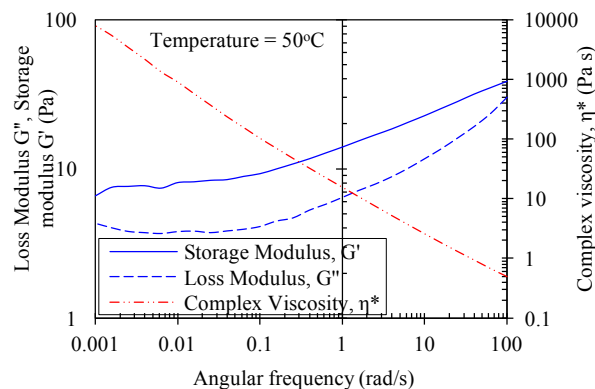


Figure 5. Frequency sweep test showing the loss and storage moduli as well as complex viscosity within the limit of LVE region.

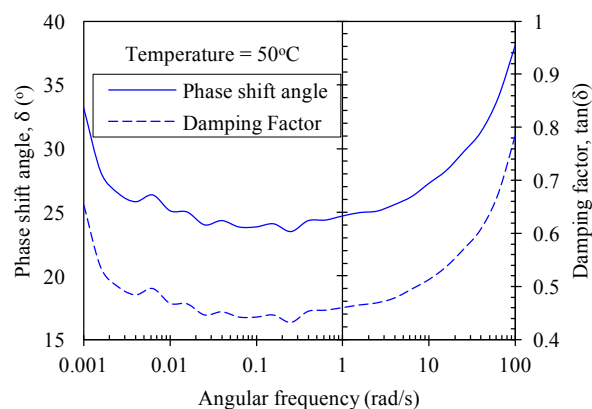


Figure 6. Frequency sweep test presented with phase shift angle and damping factor within the limit of LVE region.

### Dynamic sag analysis

Viscosity measurements as a function of time for fixed shear rates are presented in Fig. 7. For constant shear rates of 5.11, 1.703, and  $0.10 \text{ s}^{-1}$ , there is a sudden decrease in viscosity within the first 100 – 200 s, followed by a gradual increase in viscosity until a steady state condition is reached. Nonetheless, for a shear rate of  $0.001 \text{ s}^{-1}$ , a sharp increase in viscosity is recorded over the first 500 s, after which a gradual increase in viscosity is observed. The average fluid viscosity is recorded for each shear rate within the time range of 3000 – 4000 s. The larger the shear rate, the lower the steady-state viscosity. This implies that larger shear rates indicate larger shear stresses, which

result in dramatic breakdown of the fluid's microstructure. The recorded viscosities are 599.24, 17.10, 1.49, and 0.62 Pa s for shear rates of 0.001, 0.10, 1.703, and 5.11 s<sup>-1</sup> respectively. Furthermore, in Fig. 7, as the shear rate increases, the time required for the steady-state viscosity to be reached is drastically decreased. This implies that a sizable thixotropic effect is displayed at low shear rates where more time is required to achieve steady-state, whereas, no thixotropic effect occurs at high shear rates as indicated by very short time required to achieve steady-state.<sup>14</sup>

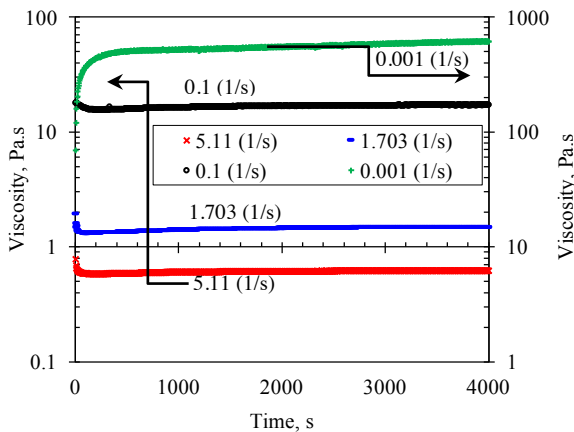


Figure 7. Constant shear rate time sweep test for the sample fluid system at 50°C showing steady-state condition.

The dynamic sag and sag factor are plotted against the shear rate and presented in Fig. 8 and Fig. 9 respectively. It is observed that both dynamic sag and sag factor decline as shear rate decreases due to less structural breakdown of the drilling fluid. Besides, the fluid sample viscosity decreases with increasing shear rate. With higher viscosity, less dynamic sag and sag factor are observed. Similar phenomenon was earlier reported by Saasen et al.,<sup>2</sup>. The drilling fluid sample exhibited acceptable suspension characteristics with a sag factor between 0.50 to 0.53. This however allows for some expected and unavoidable settling of barite particles.<sup>12</sup>

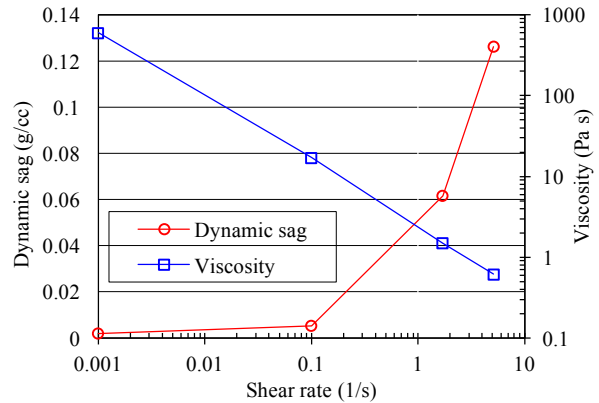


Figure 8. Dynamic sag test presented with average fluid viscosity for variable shear rate at 50°C.

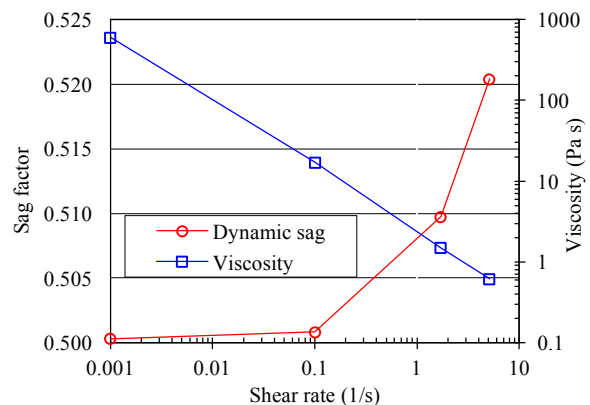


Figure 9. Sag factor presented with average fluid viscosity for variable shear rate at 50°C.

Oscillatory shear test results are shown in Fig. 10. As the storage modulus  $G'$  reflects the elastic behaviour of the fluid sample, the loss modulus  $G''$  and  $\tan(\delta)$  also define respectively the viscous behaviour and gel properties of the fluid sample. Typically, during gel growth for drilling fluids,  $\tan(\delta)$  value will initially decrease sharply over the first few minutes indicating the growth of structural dominance of the fluid, and then continue to decrease before levelling out.<sup>13</sup> Any increase in  $\tan(\delta)$  or  $G''$  or decrease in  $G'$  afterwards is indicative of changes in gel structure and/or settling of barite particles. According to Fig. 10, there is initially a significant structural buildup as  $\tan(\delta)$  decreases and  $G'$  increases over the first 1000 s. However, above 1000 s,  $\tan(\delta)$  increases

rapidly as  $G''$  also increases. These phenomena indicate that there is a breakdown of the fluid's gel structure which is evidenced by barite particle settling.

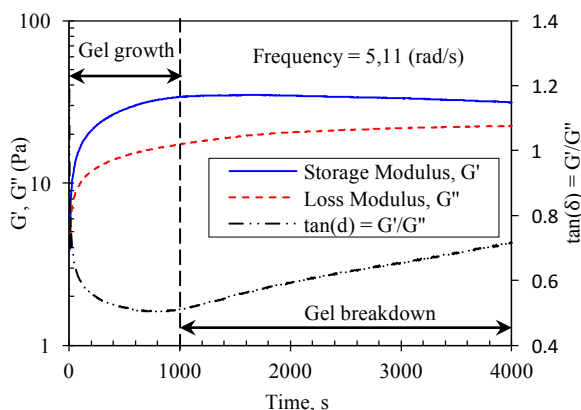


Figure 10. Oscillatory time sweep testing presented with storage and loss moduli, and damping factor at 50°C.

## CONCLUSIONS

This study has presented an indirect approach to analyse dynamic barite sag for an oil-based drilling fluid sample. The following conclusions can be drawn from this study:

1. Dynamic sag is predictable based on the rheometer measurements.
2. As the fluid viscosity increases with decreasing shear rate, dynamic sag becomes less pronounced.
3. There is a strong dependence of barite sag on shear rate above a critical shear rate value of  $0.1 \text{ s}^{-1}$ .
4. Oscillatory time sweep test gives a good indication of dynamic sag potential.

## ACKNOWLEDGMENTS

The authors wish to thank M-I SWACO for providing the drilling fluid chemicals.

## REFERENCES

1. Zamora, M., and Jefferson, D. 1994. "Controlling Barite Sag Can Reduce Drilling Problems", *Oil & Gas Journal* (92) 47-52.
2. Saasen A., Liu, D., Marken, C.D., Sterri, N., Halsey, G.W., and Isambourg, P. 1995.

"Prediction of Barite Sag Potential of Drilling Fluids from Rheological Measurements", SPE/IADC Number 29410, Presented at the *SPE/IADC Drilling Conference*, Amsterdam, 28 February – 2 March.

3. Tehrani, A., Zamora, M., and Power, D. 2004. "Role of Rheology in Barite Sag in SBM and OBM", *AADE Drilling Fluids Conference*, Houston Texas, April 6-7.

4. Skalle P., Backe, K.R., Lyomov, S.K., and Sveen, J. 1999. "Barite Segregation in Inclined Boreholes", *Journal of Canadian Petroleum Technology* (38) 13.

5. Omland, T.H., Saasen, A., and Amundsen, P.A. 2007. "Detection Techniques Determining Weighting Materia Sag in Drilling Fluid and Relationship to Rheology", *Annual Transactions of the Nordic Rheology Society* (15) 1-9.

6. Dye, W., Hemphill, T., Gusler, W., and Mullen, G. 2001. "Correlation of Ultralow-Shear-Rate Viscosity and Dynamic Barite Sag", *SPE Drilling & Completion* (16) 27-34.

7. Jamison, D.E., and Clements, W.R. 1990. "A New Test Method to Characterize Setting/Sag Tendencies of Drilling Fluids Used in Extended Reach Drilling", *ASME Drilling Technology Symposium* (27) 109-113.

8. Marshall, D.S. 2007. "Laboratory Investigation of Barite Sag in Drilling Fluids", *Annual Transactions of the Nordic Rheology Society* (15).

9. Savari, S., Kulkarni, S., Maxey, J., and Teke, K. 2013. "A Comprehensive Approach to Barite Sag Analysis on Field Muds", *AADE National Technical Conference and Exhibition*, Cox Convention Centre, Oklahoma City, February 26-27.

10. Mezger, T.G. 2014. *The Rheology Handbook*. 4ed. Vincentz Network, Hannover, Germany.

11. Hold, S. 2015. "The Very Basics of Density Measurement Methods", *Anton Paar Blog*. <https://blog.anton-paar.com/the-very-basics-of-density-measurement/>.



12. Maxey, J. 2007. "Rheological Analysis of Static and Dynamic Sag in Drilling Fluids", *Annual Transactions of the Nordic Rheology Society* (15) 181-188.

13. Maxey, J. 2006. "Rheological Analysis of Oilfield Drilling Fluids", *AADE Drilling Fluids Technical Conference*, Houston Texas, April 11-12.

14. Varges, P.R., Costa, C.M., Fonseca, B.S., Naccache, M.F., and De Souza Mendes, P.R. 2019. "Rheological Characterization of Carbopol Dispersions in Water and in Water/Glycerol Solutions", *Fluids* (15) 3.